Ecosystems
DOI: 10.1007/s10021-015-9918-1

ECOSYSTEMS

Metabolism, Gas Exchange, and Carbon Spiraling in Rivers

Robert O. Hall Jr.,[1]* Jennifer L. Tank,[2] Michelle A. Baker,[3] Emma J. Rosi-Marshall,[4] and Erin R. Hotchkiss[5,6]

[1]*Department of Zoology and Physiology, University of Wyoming, Laramie, Wyoming 82071, USA;* [2]*Department of Biological Sciences, University of Notre Dame, Notre Dame, Indiana 46556, USA;* [3]*Department of Biology and Ecology Center, Utah State University, Logan, Utah 84322, USA;* [4]*Cary Institute of Ecosystem Studies, Box AB, Millbrook, New York 12545, USA;* [5]*Program in Ecology and Department of Zoology and Physiology, University of Wyoming, Laramie, Wyoming 82071, USA;* [6]*Present address: Département des sciences biologiques, Université du Québec à Montréal, Montréal, Québec, Canada*

Abstract

Ecosystem metabolism, that is, gross primary productivity (GPP) and ecosystem respiration (ER), controls organic carbon (OC) cycling in stream and river networks and is expected to vary predictably with network position. However, estimates of metabolism in small streams outnumber those from rivers such that there are limited empirical data comparing metabolism across a range of stream and river sizes. We measured metabolism in 14 rivers (discharge range 14–84 $m^3\ s^{-1}$) in the Western and Midwestern United States (US). We estimated GPP, ER, and gas exchange rates using a Lagrangian, 2-station oxygen model solved in a Bayesian framework. GPP ranged from 0.6–22 g $O_2\ m^{-2}\ d^{-1}$ and ER tracked GPP, suggesting that autotrophic production supports much of riverine ER in summer. Net ecosystem production, the balance between GPP and ER was 0 or greater in 4 rivers showing autotrophy on that day. River velocity and slope predicted gas exchange estimates from these 14 rivers in agreement with empirical models. Carbon turnover lengths (that is, the distance traveled before OC is mineralized to CO_2) ranged from 38 to 1190 km, with the longest turnover lengths in high-sediment, arid-land rivers. We also compared estimated turnover lengths with the relative length of the river segment between major tributaries or lakes; the mean ratio of carbon turnover length to river length was 1.6, demonstrating that rivers can mineralize much of the OC load along their length at baseflow. Carbon mineralization velocities ranged from 0.05 to 0.81 m d^{-1}, and were not different than measurements from small streams. Given high GPP relative to ER, combined with generally short OC spiraling lengths, rivers can be highly reactive with regard to OC cycling.

Key words: rivers; gross primary production; Ecosystem respiration; carbon spiraling; gas exchange; ecosystem metabolism.

Introduction

There is a renewed interest in carbon cycling in freshwater ecosystems as ecologists link metabolic processes with regional carbon (C) budgets (Battin and others 2009; Tranvik and others 2009), but empirical measurements of metabolism in a wide variety of freshwater ecosystems are lacking, as is

Received 3 June 2015; accepted 18 July 2015

Electronic supplementary material: The online version of this article (doi:10.1007/s10021-015-9918-1) contains supplementary material, which is available to authorized users.

Author Contributions ROH designed the study, conducted fieldwork, analyzed data, and wrote first draft of the paper. JLT, MAB, and EJR-M designed the study, conducted fieldwork, and wrote the paper. ERH conducted field and lab work and wrote the paper.

*Corresponding author; e-mail: bhall@uwyo.edu

Published online: 28 September 2015

our understanding of processes that control variation within and across ecosystems. Ecosystem size and position in the landscape will control variation in rates of C supply and in situ metabolism; for example, lake size correlates with metabolism (Staehr and others 2012). In the case of streams and rivers, ecosystem processes such as C cycling will vary both as a function of size (as volumetric flow) and landscape position, given that the downstream movement of water connects headwaters with larger streams and rivers (Webster 2007). The effects of stream size and landscape position on C cycling were initially conceptualized as part of the River Continuum Concept (RCC) where headwater streams were predicted to have high rates of ecosystem respiration (ER) relative to gross primary production (GPP), whereas mid-order reaches were predicted to have higher GPP relative to ER because of increased light availability supporting autochthony combined with reduced allochthonous inputs of C (Vannote and others 1980). In contrast, large rivers with high sediment loads would revert to a pattern of higher ER relative to GPP, like headwater streams, because of decreased light penetration in the water column combined with the import of allochthonous particles from upstream. Data from selected river continua have supported the pattern of increasing GPP/ER downstream from headwaters to non-wadeable rivers (Meyer and Edwards 1990; McTammany and others 2003).

Despite strong conceptual foundations and limited empirical data on how larger streams and rivers function, metabolism estimates in rivers are far fewer in number than those from small streams. Only 10% of reach-scale metabolism estimates (reviewed below) have been conducted in rivers with discharge greater than 10 $m^3 s^{-1}$ (~20 m width), whereas greater than >50% have been made in streams less than 0.1 $m^3 s^{-1}$. Recent advances for estimating gas exchange from dissolved oxygen (O_2) data (Holtgrieve and others 2010; Dodds and others 2013) make estimating metabolism in rivers potentially as straightforward as in small streams. In addition, understanding variation and controls on metabolism in rivers will allow ecologists to answer a variety of unanswered questions in river networks. For example, river food webs are based to a large degree on in situ primary production (Thorp and Delong 2002; Cross and others 2013), but there are few data on the actual rates of primary production in rivers.

More broadly, ecosystem metabolism in rivers is of general interest because of the potential for rivers to store, mineralize, and transport terrestrial organic carbon (OC) before reaching the coastal zone (Battin and others 2008; Raymond and others 2013). It is well known that small streams can respire large quantities of terrestrial OC (Marcarelli and others 2011), yet the role of rivers is less understood, despite evidence showing that big rivers also transform terrestrial OC (Cole and Caraco 2001). Riverine metabolism estimates will also facilitate the calculation of OC spiraling lengths (Newbold and others 1982), allowing further comparison among small streams and larger rivers. The OC spiraling method examines downstream C flux relative to mineralization and is a direct estimate of the degree to which rivers mineralize versus transport OC. Oddly, ecosystem ecologists rarely use this spiraling metric to describe the role of streams and rivers in C cycling despite strong theoretical (Webster 2007) and empirical (Thomas and others 2005; Taylor and others 2006; Griffiths and others 2012) examples.

Here, we measured metabolism of 14 rivers ranging in size from 14 to 84 $m^{-3} s^{-1}$ to link metabolism metrics with OC cycling. We had 3 objectives: (1) develop a two-station model, solved via Bayesian inverse modeling of metabolism parameters, to measure metabolism in each of 14 rivers varying in physical attributes in Midwest and Western US; (2) combine riverine metabolism values with others from the literature to examine how the balance of GPP and ER varies across a large size range of streams and rivers; and (3) calculate instantaneous metrics of OC spiraling to estimate the degree to which river reaches can process OC.

Methods

Study Sites

We chose 14 rivers in the Midwest and Western US that varied chemically, physically, and geomorphically (Table 1, Online Appendix 1). This study was part of a larger study investigating nutrient cycling in rivers; thus, we chose sites to maximize variation in suspended sediment and nutrient concentrations. Sites in western Wyoming and eastern Idaho had low nutrient and low suspended sediment concentrations, central Wyoming and Utah rivers had low to medium nutrient concentrations and medium to high suspended sediments, and Midwestern rivers had generally higher nutrients and low to medium suspended sediments (Table 1). We chose the study reaches by taking into consideration the proximity of bridges for adding solutes, the presence of USGS gages for measurements of discharge, and the presence of

Table 1. Physical and Chemical Properties and Metabolism of the 14 Rivers in This Study

River	Discharge ($m^3\ s^{-1}$)	Width (m)	Velocity ($m\ min^{-1}$)	Mean depth (m)	NH_4^+ ($\mu g\ N\ L^{-1}$)	NO_3^- ($\mu g\ N\ L^{-1}$)	SRP ($\mu g\ P\ L^{-1}$)	Turbidity (fnu)	GPP ($g\ O_2\ m^{-2}\ d^{-1}$)	ER ($g\ O_2\ m^{-2}\ d^{-1}$)	K_{600} (d^{-1})
Buffalo Fork	19.1	35.2	55.8	0.58	5	3	44	3	0.8 (0.7, 0.8)	−3.4 (−3.5, −3.3)	8.7 (8.5, 8.9)
Green River, WY	25.5	62.5	32.4	0.76	5	15	21	3	19.9 (18.3, 21.5)	−17.5 (−20.0, −15.0)	8.3 (6.5, 10.0)
Henry's Fork	69.6	62.0	61.7	1.09	3	6	16	1	22.1 (20.6, 23.6)	−18.1 (−20.2, −15.9)	15.6 (13.9, 17.3)
Snake River	71.7	65.3	63.4	1.04	5	bd	7	0	3.0 (2.9,3.1)	−5.1 (−5.6, −4.7)	7.0 (7.0, 7.0)
Salmon River	25.9	50.5	59.2	0.52	5	2	4	2	4.0 (3.9,4.2)	−5.1 (−5.8, −4.7)	15.2 (14.2, 16.4)
Tippecanoe River	19.0	50.6	37.9	0.59	15	1850	67	17	2.6 (2.5, 2.7)	−5.3 (−5.4, −5.2)	2.1 (2.0, 2.3)
East Fork, White River	14.0	47.9	21.4	0.82	1	1650	60	43	4.7 (4.4, 5.0)	−5.6 (−5.6,−5.5)	1.7 (1.6, 1.8)
Muskegon River	33.0	67.0	28.3	1.05	14	330	9	23	3.0 (3.0, 3.0)	−4.8 (−4.8, −4.7)	3.0 (3.0, 3.1)
Manistee River	36.5	52.5	33.4	1.25	30	120	10	3	3.9 (3.5,4.2)	−4.4 (−4.6, −4.2)	2.0 (1.9, 2.1)
North Platte River	83.9	81.3	58.9	1.05	5	20	20	19	4.0 (3.7,4.5)	−6.8 (−7.6, −6.1)	4.4 (4.0, 4.9)
Bear River	16.0	37.3	26.6	0.97	12	49	18	53	1.1 (1.0,1.3)	−1.1 (−1.6, −0.7)	0.5 (−0.5,1.6)
Green River at Ouray	37.9	111.8	31.6	0.64	2	7	3	16	1.1 (1.1,1.2)	−1.2 (−1.5, −1.0)	2.1(1.7, 2.6)
Green River at Gray Canyon	41.0	79.1	23.2	1.34	14	19	22	607	0.3 (0.2, 0.5)	−3.0 (−3.1, −2.9)	2.1 (2.0, 2.2)
Colorado River	63.4	83.1	34.3	1.33	1	697	12	116	4.5 (4.3, 4.8)	−2.7 (−3.3, −2.2)	6.3 (6.2,6.5)

Values in parentheses represent 95% bootstrap confidence intervals for metabolism based on 2–8 metabolism estimates at each site.

boat ramps for reach-scale sampling logistics. Rivers varied in summer baseflow discharge from 14 to 84 $m^3\ s^{-1}$ with an average of 39 $m^3\ s^{-1}$.

Field and Laboratory Methods

At most sites, we performed two-station metabolism estimates based on sampling dissolved O_2 through time. We used 1–2 sondes to measure dissolved O_2 at each of 2 stations for 2 days giving us 2–8 estimates of metabolism. We anchored 2–4 multi-parameter Hydrolab Minisondes equipped with optical O_2 sensors in areas of moderate downstream flow, at stations 2.5–10.7 km apart (mean 6.1 km) along each river, with mean distance between sondes corresponding to an average of 2.7 h of travel time. We calibrated the sondes river-side in a 100-L pot of air-saturated water that we vigorously bubbled using an aquaculture air pump and air stone. This method of bubbling oversaturates O_2 by 2%. Bubbling this pot in the laboratory and measuring Ar (which has similar diffusivity as O_2) on a membrane-inlet mass spectrometer, we found that Ar was 2% (±0.15%) oversaturated. This phenomenon is likely due to oversaturation due to bubble-mediated gas exchange (for example, Hall and others 2012). We corrected our oxygen data downwards by 2% to counter this over calibration. Following initial calibration, we recorded O_2 readings in this air-saturated water to check calibration and that all sondes remained within 2% of saturation; O_2 readings from sondes drifted little during the deployments and thus did not need drift correction. We recorded O_2, temperature, and turbidity using these sondes at 5-min intervals during 3-d deployments during summer baseflow conditions (that is, July or August).

We also collected physical and chemical data at each site; discharge (Q, $m^3\ s^{-1}$) came from nearby USGS gaging stations or gages associated with upstream dams. We measured wetted channel width (w, m) of the reach at approximately 70 locations throughout the study reach using a laser rangefinder operated from a boat. We also conducted solute tracer additions as part of nutrient uptake experiments, adding Rhodamine WT (RWT) and NaBr in separate pulse additions with target downstream concentrations of 10 μg RWT L^{-1} or 50 μg $Br^-\ L^{-1}$. We monitored RWT at 4 stations downstream of the release point using 4 Hydrolab Minisondes equipped with fluorometric sensors programed to record RWT concentration every 10 s, while Br^- samples were manually collected from the river thalweg at timed intervals and analyzed using ion chromatography (Dionex models ICS-5000) using US-EPA standard method 300.0. These tracer releases were used to calculate nominal travel time (that is, the time for 50% of the solute to pass the downstream station), and mean velocity (V, m min^{-1}) was then calculated as reach length/nominal travel time, while mean depth (z, m) was estimated based on continuity, $z = Q/(wV)$. We also measured background water column nutrients at each site as part of the nutrient uptake experiments and reach-scale estimates were based on the average of 3–5 samples collected at 4 sites. We analyzed NH_4^+-N using the phenol-hypochlorite method (Solorzano 1969), NO_3^--N using the cadmium reduction method (APHA 1998), and SRP using the ascorbic acid method (Murphy and Riley 1962) on a Lachat Flow Injection Autoanalyzer (Lachat Instruments, Loveland, CO, USA).

To estimate C spiraling, we sampled particulate OC (POC) and dissolved OC (DOC). We collected POC from 3 grab samples taken in the thalweg at 4 locations from each river. Rivers averaged 0.6–1.3 m deep and were turbulent; hence, we did not take depth-integrated samples. For POC, we immediately filtered a known volume of water in the field onto pre-ashed and weighed glass fiber filters (Whatman GF/F), air dried the filters and stored them for transport to the lab where we dried them at 60°C, weighed them, and combusted at 500°C. We reweighed the filters to obtain an ash-free dry mass (AFDM) and converted to mg AFDM/L given the volume of sample filtered; we assumed that 50% 0f AFDM was C. Samples for DOC came from triplicate samples at one location. These were filtered with pre-ashed glass fiber filters (Whatman GF/F), acidified with HCl to a pH of 2, and then stored in acid washed and ashed borosilicate amber vials (I-Chem, 40 mL). We transported samples on ice to the laboratory, and refrigerated them until analysis on a Shimadzu Total Organic Carbon Analyzer (TOC-5000A; measurement precision of ±0.05 mg C L^{-1}).

Metabolism Estimation

We estimated metabolism and gas exchange by fitting a two-station Lagrangian model to the dissolved O_2 data, except for the Muskegon, North Platte, and Bear rivers where we used a one-station method due to instrument failures or burial of the upstream sondes. A two-station procedure measures metabolism in a defined reach of river between the upstream and downstream O_2 sensors, which allows estimation of reach-scale metabolism, even below river discontinuities, such as dams,

which may be included in the upstream footprint of one-station O_2 measurements. A general model for two-station metabolism is:

$$Odown_{(t+\tau)} = Oup_{(t)} + \mathrm{GPP} + \mathrm{ER} + \text{gas exchange}, \tag{1}$$

where $Oup_{(t)}$ is the upstream O_2 concentration (g O_2 m^{-3}) and $Odown_{(t+\tau)}$ is downstream O_2 concentration of that same parcel of water following travel time, τ. GPP and ER are both expressed in g O_2 m^{-2} d^{-1}, and represented as positive and negative rates of O_2 production and consumption, respectively.

An expansion of this model is

$$Odown_{(t+\tau)} = Oup_{(t)} + \left(\frac{\mathrm{GPP}}{z} \times \frac{\sum_t^{t+\tau} \mathrm{PPFD}}{\mathrm{PPFD_{total}}}\right) + \frac{\mathrm{ER}}{z}\tau + K\tau\left(\frac{Osatup_{(t)} + Osatdown_{(t+\tau)}}{2} - \frac{Oup_{(t)} + Odown_{(t+\tau)}}{2}\right), \tag{2}$$

where z is mean depth (m), and *Osatup* and *Osatdown* are O_2 saturation concentrations upstream and downstream (g O_2 m^{-3}). Gas exchange flux was the gas exchange rate, K (d^{-1}) multiplied by the dissolved O_2 saturation deficit, which we averaged for the upstream and downstream stations. We use light to drive GPP in this model (Van de Bogert and others 2007). For any parcel of water, the fraction of light it accumulates is the sum of the photosynthetic photon flux density (PPFD, μmol m^{-2} s^{-1}) accumulated in the time interval from t to ($t + \tau$) divided by the daily total of PPFD ($\mathrm{PPFD_{total}}$). Equation 2 has *Odown* on both sides; we need *Odown* on the left side of the equation because we are comparing modeled *Odown* with the data. Following some algebra we get

$$Odown_{(t+\tau)} = \frac{Oup_{(t)} + \left(\frac{\mathrm{GPP}}{z} \times \frac{\sum_t^{t+\tau} \mathrm{PPFD}}{\mathrm{PPFD_{total}}}\right) + \frac{\mathrm{ER}}{z}\tau + K\tau\left(\frac{Osatup_{(t)} - Oup_{(t)} + Osatdown_{(t+\tau)}}{2}\right)}{1 + \frac{K\tau}{2}}. \tag{3}$$

Assumptions of this model are that GPP is a linear function of light intensity, ER is constant throughout the day, and that the average of up and down station O_2 saturation deficit is representative for the entire reach. We tested the assumption of linear light relationships by using 1-station models (equation 4 below) for 1 day on each river with a Jassby–Platt light saturation function exactly following Holtgrieve and others (2010). Eight of 14 rivers had linear light response curves. Six showed slightly curvilinear relationships, with increase in GPP 3-10%, with a concomitant twofold increase in the credible intervals. In a two-station model with 3-h travel times, it would be necessary to divide these travel times into 5-min intervals to calculate and sum GPP for each. We felt that a potential increase in accuracy of 10% for 6 of the rivers did not warrant this increased model complexity. We did not include a diel temperature response for ER because the relationship of ER to temperature is highly variable (Huryn and others 2014; Jankowski and others 2014), and thus, we would have needed to estimate this parameter in addition to GPP, ER, and K, possibly producing an overfitted model. Gas exchange is estimated as K_{600} (d^{-1}) and is corrected for temperature at each time step based on Schmidt number scaling (Jähne and Haußecker 1998). We convert this per time rate to a gas exchange velocity (k_{600}, m/d) by multiplying by mean depth, z, to facilitate comparisons with published gas exchange velocities. We used modeled solar insolation data for equation 3 based on geographic location and time of day and year.

For the 3 rivers using a one-station method (North Platte, Bear, and Muskegon), we used the following model (Van de Bogert and others 2007):

$$O_t = O_{t-\Delta t} + \frac{\mathrm{GPP}}{z} \times \frac{\mathrm{PPFD}_t}{\mathrm{PPFD_{total}}} + \frac{\mathrm{ER}}{z}\Delta t + K\Delta t(Osat_{t-\Delta t} - O_{t-\Delta t}), \tag{4}$$

where t is time of day and Δt is the time between O_2 measurements. This model measures O_2 change in one place rather than tracking it downstream and in a longitudinally homogenous river, one-station analyses will give the similar results to a two-station model (Reichert and others 2009). Of the 3 rivers, only the Muskegon had a dam located 47 km upstream, but we suggest that its influence was negligible because the dam was located twice the distance (1.6 V/K) for 80% of O_2 turnover (Chapra and Di Toro 1991).

Based on the above models, we used a Bayesian inverse modeling procedure to estimate metabolism (GPP and ER) and gas exchange rate (K_{600}) roughly following Holtgrieve and others (2010). Bayesian analysis treats parameters as random variables with a corresponding probability distribution and allows estimating uncertainty for the modeled parameters. Because we solved for gas exchange as well as GPP and ER, there is the risk of overfitting the model, and posterior probability distributions solved via a Bayesian approach allowed us to examine this assumption closely. At all but one sites we had two full days of data, and we fit each daytime period separately starting at 22:00 the night before to 06:00 the day after for a total of 32 h.

Following Bayes rule, we calculated the posterior probability distribution of the parameters as

$$P(\theta|D) \propto P(D|\theta) \times P(\theta), \tag{5}$$

where θ is a vector of parameters, GPP, ER and K, and D is the O_2 data for the downstream or single station. The likelihood of the data given θ assumes normally distributed error and is calculated as

$$\mathscr{L}(D|\theta) = \prod_{i=1}^{n} N\left(D_i|\mu_i, \sigma_i^2\right), \tag{6}$$

where the likelihood of D given θ is the product of likelihoods of the data relative to modeled downstream O_2 concentrations (μ_i,) and variance (σ_i^2). We simulated the posterior distribution $P(\theta|\mathrm{D})$ using a Metropolis algorithm and Markov-chain Monte Carlo (MCMC) using function *metrop* in the *mcmc* package for R (Geyer and Johnson 2013, R Development Core Team 2011). We ran each chain for 20,000 iterations following burn-in and we started all MCMC chains with different parameter values to ensure a global solution. We did not thin chains and we adjusted the proposal distribution of the Metropolis algorithm to achieve an acceptance rate near 20%. For metabolism parameters, we used minimally informative prior probability distributions (GPP $\sim N$ ($\mu = 5$, SD = 10), ER $\sim N$ ($\mu = -5$, SD = 10). For gas exchange, we used the nighttime regression method (Hornberger and Kelly 1975) or empirical equation 7 from Raymond and others (2012) to assign a normal prior probability distribution, where the mean and standard deviation of the prior probability distribution were the mean and standard deviation, respectively, of the 4 slopes from nighttime regression measured by the two O_2 sondes over two nights or the error in the predictive equation. Code for one- and two-station models is in Online Appendix 5.

Calculation of C Spiraling

We calculated turnover length of OC for each river following (Newbold and others 1982) where spiraling length (S_{OC}, m) is the ratio of downstream transport relative to mineralization and is calculated as

$$S_{OC} = \frac{Q \times [OC]}{-HR \times w}. \tag{7}$$

Discharge (Q) and stream width (w) were estimated as described above, and the sum of POC and DOC gives the organic C concentration [OC]. However, to calculate S_{OC} requires an estimate of heterotrophic respiration (HR, which is a negative flux) that equals ER—AR, where AR is the respiration by algae and macrophytes themselves. Typically, researchers assume that AR is some fraction of GPP (for example, 0.2–0.5) but a recent analysis suggests that the daily fraction of GPP (AR_f) consumed by respiration by algae is about 44% (Hall and Beaulieu 2013). Assuming this fraction, we estimated HR as

$$HR = ER - AR_f \times GPP. \tag{8}$$

Turnover length of OC will depend strongly on the size of the river. To compare mineralization relative to [OC] (that is, [DOC] + [POC]), we calculated a ''mineralization velocity'' (v_{f-OC}, m d^{-1}) of OC as

$$v_{f-OC} = \frac{-HR}{[OC]} \tag{9}$$

analogous to uptake velocity measured in nutrient uptake studies (Hall and others 2013). We converted HR in O_2 units to g C m^{-2} d^{-1} by assuming a 1:1 molar relationship between C and O in respiration and we then compared v_{f-OC} to those measured in other rivers and streams where OC spiraling length was reported. Error in not perfectly knowing AR_f may introduce error into estimates of v_{f-OC}. Therefore, we calculated v_{f-OC} 1000 times with each replicate using a randomly selected estimate of AR_f from Hall and Beaulieu (2013) and 3 subsequent studies (Roley and others 2014; Genzoli and Hall, unpublished data; Hall and others, unpublished data). Finally, we compared S_{OC} to the estimate of river length estimated from GIS; we defined the segment distance for each river as the length of river downstream of a major reservoir or confluence of large tributary and upstream of a lake, reservoir, or much larger river. This designation of river length was not meant as a definition, but rather to provide some context for considering OC turnover length, S_{OC}.

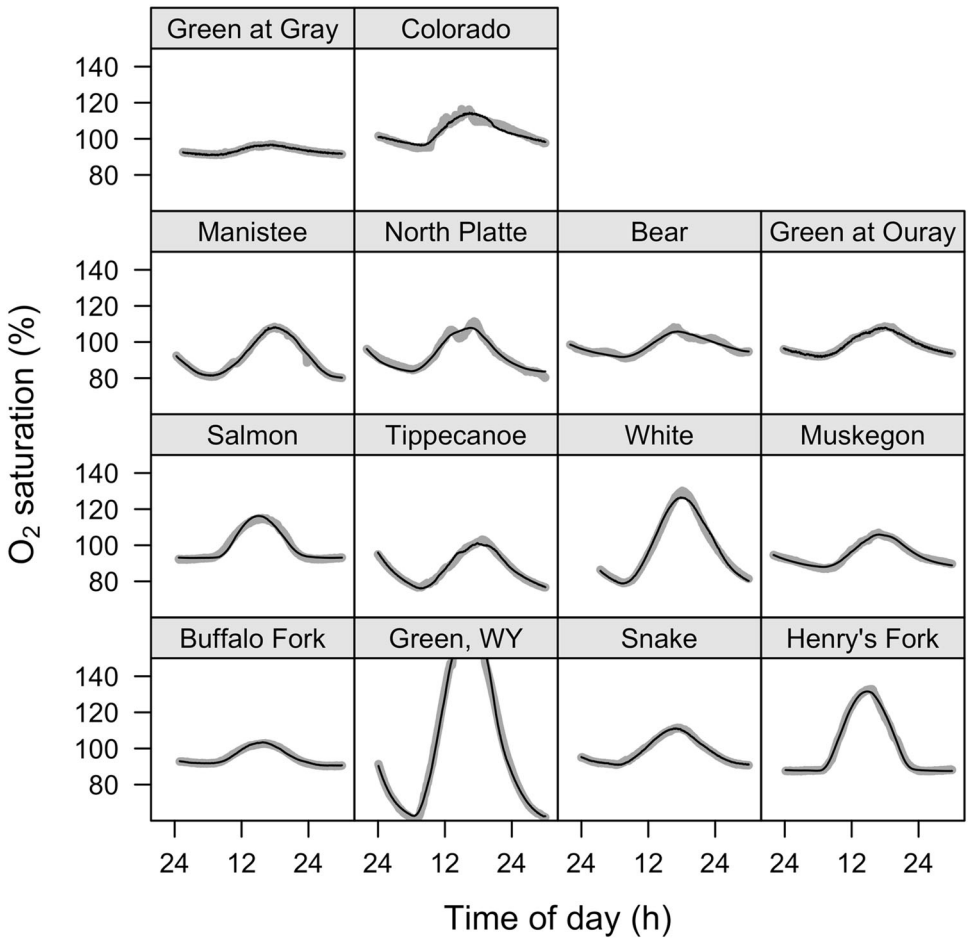

Figure 1. Data (*thick gray lines*) and model fit (*thin black line*) for 1 representative example of the 2–8 metabolism model fits for each of the 14 rivers. Each model fitting procedure was based on 1 day's worth of oxygen data. Y-axis units are % O_2 saturation to facilitate comparison among rivers.

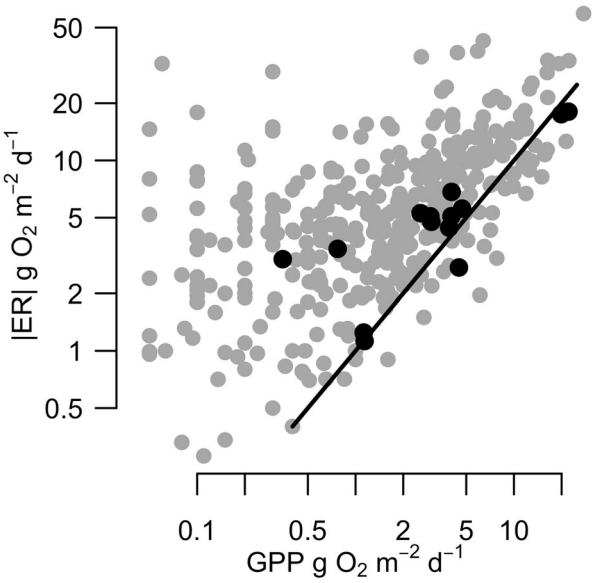

Figure 2. Gross primary production (GPP) versus ecosystem respiration (ER) for our 14 rivers (*black points*) and other data (*gray circles*) show high variation among studies. Line is GPP = ER. Axes are log scaled.

Statistical Inference

We used Pearson correlations to relate rates of metabolism to predictor variables, and rates of C spiraling to river size. Inference on this correlation coefficient (r) was based on calculating default Bayes factors for correlation (Wetzels and Wagenmakers 2012), which can be interpreted as the relative probability that a linear relation exists between 2 variables. Bayes factors greater than 6 constitute strong evidence in support of the alternative hypothesis (linear relation) versus a null. We estimated error on metabolism estimates, GPP, ER and K_{600}, not as the parameter error from the MCMC solutions, but rather on the bootstrap 95% confidence intervals from the 2–8 metabolism estimates (that is, the median value of the posterior probability distributions) at each site. This approach assumes no within-estimate error, which follows the fact that the among-estimate error exceeded the parameter error from any one MCMC solution. We performed all statistics using R (R Development Core Team 2011).

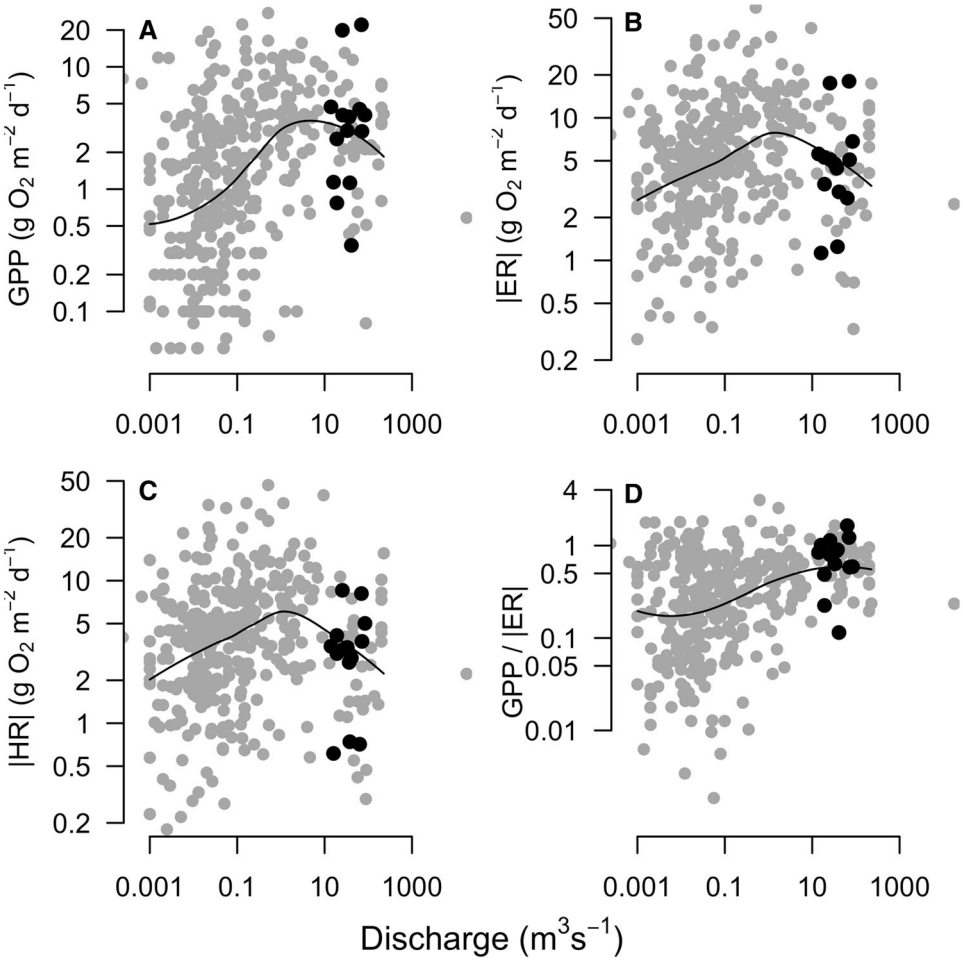

Figure 3. Gross primary production (GPP) (**A**), Ecosystem respiration (|ER|) (**B**), Heterotrophic respiration (|HR|) (**C**), and GPP/|ER| (**D**) as a function of river discharge. *Black points* are the 14 rivers from this study, gray are other data. Axes are log scaled. *Lines* are locally weighted regression with smoothing factor = 0.75. The point far to the right is from the Mississippi river and represents the largest possible size for a North American river (Dodds and others 2013). Because of the zero density in points between the Mississippi River and the second largest river in the dataset, we did not fit the regression line to the Mississippi River.

We compared rates of metabolism in this study to those from many other streams and rivers, collating estimates of reach-scale, open channel metabolism from Marcarelli and others (2011). We also added newer studies to this dataset, of which several are from similar-sized rivers as the ones studied here (Online Appendix 4). We used locally weighted regression (Trexler and Travis 1993) with a smoothing parameter of 0.75 to visualize trends in metabolism as a function of river discharge.

Results

Models fit the data closely and had low error in estimates of the parameters, GPP, ER, and *K* (Figure 1). The 95% credible interval on metabolism parameters for any model fit averaged less than 10% of the of value of the parameter itself (Table 1). Variation in parameter estimates between the two measurement days or among sondes was higher than credible intervals within any one day (Table 1, Online Appendix 2).

GPP and ER varied strongly among the 14 rivers (Table 1; Figure 2); variation in GPP ranged from 0.6 to 22 g O_2 m^{-2} d^{-1}, and encompassed much of the range of GPP measured previously in small streams. However, for these rivers, unlike many smaller streams, GPP and ER fell closer to the 1:1 line (Figure 2) suggesting that these 14 rivers had low rates of HR relative to GPP. Neither turbidity nor nutrient concentrations correlated with GPP or ER in any of the rivers (Online Appendix 3). Nearly all Pearson correlation coefficients were less than |−0.48|, with corresponding Bayes factor of less than 0.9, which provided no support for a linear relationship between the metabolism parameters and potential covariates (Online Appendix 3). Two exceptions were benthic chlorophyll and total chlorophyll which positively correlated with ER (r = 0.76 and 0.78, respectively, with Bayes factor >27 indicating strong evidence). Log transformed GPP and |ER| were strongly positively correlated with each other (Figure 2, r = 0.74, Bayes factor = 18.6).

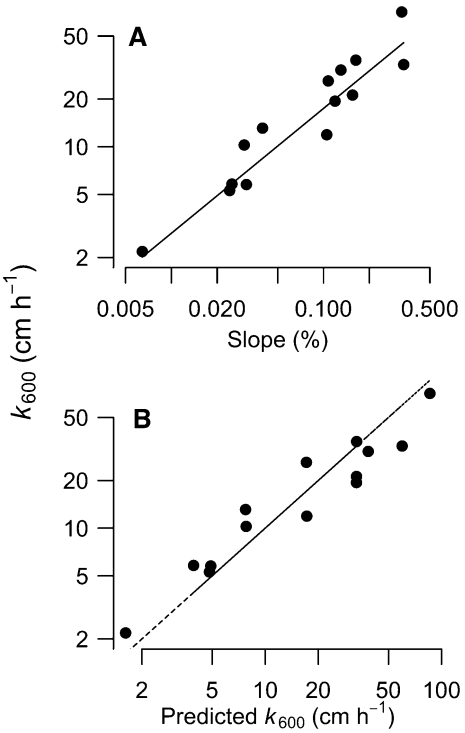

Figure 4. (**A**) Gas exchange velocity from O_2 metabolism model (k_{600}, cm h^{-1}) increased as a function of river slope (%). Line is linear regression, $\log_{10}(k_{600}) = 2.07 + 0.79 \times \log_{10}(slope)$, $r^2 = 0.89$. (**B**) Modeled gas exchange velocity lies close to that predicted by model # 7 in (Raymond and others 2012). Line is 1:1.

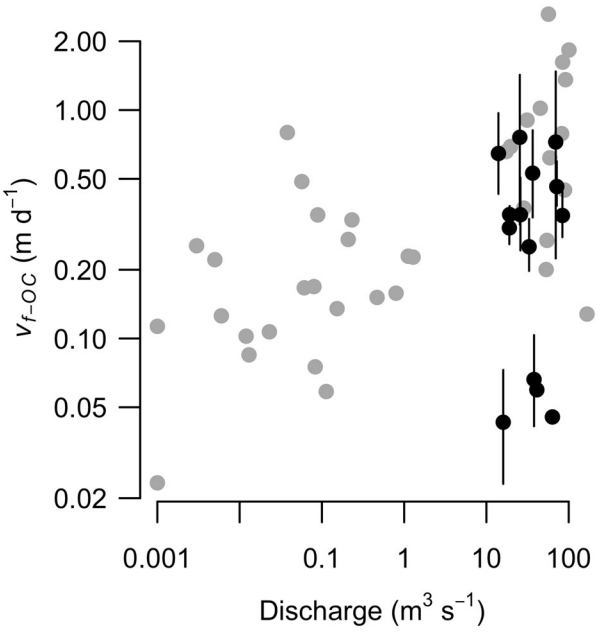

Figure 5. Mineralization velocity of organic carbon (v_{f-OC}) was positively correlated with discharge. Gray points are data from other studies, black points are 13 rivers in this study. Error bars are the 5 to 95% quantiles of v_{f-OC} calculated from a bootstrap of heterotrophic respiration (HR) from Hall and Beaulieu (2013). This error represents uncertainty in HR estimates. Pearson correlation ($r = 0.5$) and Bayes factor (127) support strong evidence for a positive relationship.

Table 2. Parameters for Estimating C Spiraling Length: Dissolved Organic C Concentration (DOC), Particulate OC Concentration (POC), and Heterotrophic Respiration (HR)

River	DOC (g m^{-3})	POC (g m^{-3})	HR (g C m^{-2} d^{-1})	S_{OC} (km)	Segment length (km)	v_{f-OC} (m d^{-1})
Buffalo Fork	2.87	0.43	1.2	134 (123, 143)	44	0.351
Green River, WY	3.64	0.39	3.3	43 (25, 112)	103	0.812
Henry's Fork	2.91	1.06	3.1	123 (66, 433)	120	0.787
Snake River	2.53	0.46	1.4	200 (159, 254)	136	0.473
Salmon River	3.03	0.41	1.2	123 (88, 183)	184	0.360
Tippecanoe River	4.32	0.69	1.6	104 (87, 125)	173	0.310
East Fork, White River	1.53	0.43	1.3	38 (27, 59)	246	0.672
Muskegon River	4.9	0.07	1.3	164 (127, 215)	235	0.259
Manistee River	1.74	0.10	1.0	108 (74, 177)	169	0.553
North Platte River	5.27	0.08	1.9	251 (199, 321)	217	0.354
Bear River	4.08	1.08	0.2	814 (508, 1605)	323	0.045
Green River at Ouray	3.09	0.98	0.3	422 (283, 709)	542	0.069
Green River at Gray Canyon	3.48	14.52	1.1	748 (719, 773)	542	0.060
Colorado River	2.98	2.17	0.3	1194 (403, inf)	264	0.055

S_{OC} is OC spiraling length, values in parentheses represent 5 to 95% quantiles of a bootstrap distribution from varying HR. Segment length is length of river between major upstream tributaries and larger downstream rivers or lakes. v_{fOC} is the OC mineralization velocity.

River size affected variation in metabolic rates and GPP/|ER|. GPP and ER were highly variable, but peaked in mid-sized rivers (Figure 3). Estimates of heterotrophic respiration in our 14 rivers spanned a broad range, but were not as high as some streams with less than 10 m^3 s^{-1} discharge. The ratio GPP/|ER| increased with increasing river size, and large streams and rivers did not have low values of GPP/|ER|. For example, 50% of rivers with Q less than 10 m^3 s^{-1} had GPP/|ER| less than 0.3. On the other hand, in rivers with Q greater than 10 m^3 s^{-1}, only 14% had GPP/|ER| less than 0.3.

Gas exchange (K_{600}) varied among the rivers (Table 1), with a mean of 5.7 d^{-1} and a range of 0.5–16 d^{-1}; gas exchange rates corresponded to a mean gas exchange velocity (k_{600}) of 20.8 cm h^{-1} with a range of 2–71 cm h^{-1}. Gas exchange rate was uncorrelated with river depth, but river depth only varied twofold among the 14 rivers. River slope strongly predicted gas exchange velocity (Figure 4), and k_{600} fell closely to the prediction estimate based on empirical equations used for many studies (Raymond and others 2012) (Figure 4). The 1:1 prediction line explained 84% of the variation in these 14 rivers relative to the 76% R^2 in Raymond and others (2012).

Organic C spiraling lengths (S_{OC}) averaged 319 km and ranged from 38 to 1193 km, and S_{OC} lengths were generally similar to their respective river segment lengths; median ratio of S_{OC} to segment length was 1.6 with a range of 0.2–4.7 (Table 2). Arid-land rivers with high suspended organic sediment loads and low HR (for example, Green River at two Utah sites, Colorado River, and Bear River, UT) had much longer S_{OC} than other rivers (Table 2). Mineralization velocities (v_{f-OC}) for the 14 rivers averaged 0.37 m d^{-1} and ranged from 0.05 to 0.81 m d^{-1}, and when combined with previous studies, v_{f-OC} correlated positively with discharge (r = 0.50, Bayes factor = 127, strong evidence) (Figure 5).

Discussion

Gross primary production and ER varied strongly in our 14 rivers; this variation corresponded to that of other previous measurements in similar-sized rivers. One river, the Henry's Fork, ID had among the highest GPP ever measured for a stream or river. Others, like the Bear River, UT had low rates of metabolism. The 4 rivers in the Midwestern US had moderate rates of metabolism with low variation among them. Despite evidence showing that GPP can increase as a function of stream or river size (Figure 3) (Finlay 2011), variation in metabolism among rivers was large enough that rivers have no characteristic rate of metabolism.

Because we measured metabolism on only 2 days, during summer baseflow conditions, we did not have a large within-river dataset to examine uncertainty on our estimates. As such, we used a Bayesian method that allowed us to examine parameter error within any one day (Holtgrieve and others 2010). This approach becomes necessary when solving for gas exchange as well as metabolic parameters to avoid equifinality among parameter estimates. In fact, we found low rates of parameter error. Variation between the two measurement days was higher than error estimated via computational Bayesian approach on any one day, suggesting that these within-day error estimates may not represent day-to-day error well.

GPP and ER

GPP ranged widely in our 14 rivers from among the highest rate ever measured (for example, Henry's Fork) to low rates that were similar to those measured in small, forested streams. Despite this high variability, we were unable to statistically assess controls on variation of GPP among our 14 rivers. Time series of metabolism clearly show that turbidity can control rates of GPP in a river (Hall and others 2015). We certainly expected that variation in turbidity would control GPP among rivers, but we found only weak correlation between GPP and turbidity (Online Appendix 3), even though variation in turbidity was high, suggesting that some other processes were controlling variation.

We acknowledge that we only measured metabolism for 2 days; it is very likely that antecedent conditions (for example, time since last flood) may have controlled the rates of GPP that we measured. Variation in the metabolism of one river can be as large as variation among rivers, and a strong role for antecedent conditions has been noted (Uehlinger 2006; Roberts and others 2007; Beaulieu and others 2013). One river, the Muskegon, had an unexpected dam release, tripling discharge the day before our metabolism estimates. This spate may have affected metabolism.

Despite these limitations, we can observe some anecdotal evidence for controls on GPP; for example, the rivers with the two highest rates of GPP (Green River, WY and Henry's Fork, ID) were located below water storage impoundments. Rivers below dams typically have stable flow and low turbidity and can have high benthic algal biomass with correspondingly high rates of GPP (Davis and others 2012). Henry's Fork also has substantial

inputs of groundwater-fed springs; high metabolism has been measured previously in other spring streams (Odum 1957; Hall and others 2003; Heffernan and Cohen 2010). In contrast, Buffalo Fork, WY drains mountain wilderness and is oligotrophic, and had correspondingly low rates of metabolism. However, we emphasize that we did not design the overall study to statistically tease out controls on river metabolism, but rather to assess rates and variation of riverine nutrient uptake (Tank and others, unpublished data). Statistically examining controls on metabolism would have required many more rivers (Bernot and others 2010), or we would have selected all rivers along a gradient of a predicted controlling variable, such as nutrient concentrations, in one region of the country.

GPP and ER were highly coupled in these 14 rivers (Figure 2), and unlike in some streams, we did not find high riverine ER associated with low rates of GPP. This finding suggests that despite an overall pattern of GPP/|ER| less than 1, rivers may not have extremely high rates of HR, at least during baseflow when they are not transporting large amounts of terrestrial C and GPP is high. The relationship between GPP/|ER| as a function of river discharge across the 14 rivers, combined with the full meta-analysis dataset, supports this conclusion with small streams having the potential for both low and high ratios of GPP/|ER|, whereas rivers greater than 10 m^3 s^{-1} had GPP/|ER| greater than 0.3 in 85% of the observations. Higher rates of GPP in rivers have been previously noted in other meta-analyses of stream metabolism, with the interesting twist that human perturbation has a stronger effect on metabolism in small streams relative to rivers (Finlay 2011). Studies that measure metabolism within a river network have found a similar pattern of increasing GPP/|ER| with downstream position in the network (Meyer and Edwards 1990; McTammany and others 2003); increasing GPP/|ER| with river size could be due to increasing GPP, decreasing HR, or both.

Theory predicts that lower rates of HR should occur in downstream reaches because most terrestrial (that is, allochthonous) OC inputs are mineralized in the headwaters (Webster 2007), yet HR peaks in middle river discharge (Figure 3). Rather, rivers tended to have high rates of ER, but do not have the negligible rates of GPP found frequently in small, often shaded, headwater streams (Figure 3). Alternatively, the pattern of somewhat lower HR in larger rivers may be an artifact of the rivers and time chosen for metabolism estimates. Rivers occupying a floodplain may have large spikes in HR during flooding periods (Colangelo 2007; Dodds and others 2013), which are notably not included in the 14 estimates of river metabolism that we present here. In addition, as shown by Meyer and Edwards (1990), rivers with large quantities of terrestrially derived DOC may have high rates of ER relative to GPP, though we note that they too found a pattern of increasing GPP/|ER| with increasing stream order.

Many small streams had $|ER| \gg GPP$, but we suggest that it is not possible to have $GPP \gg |ER|$ because of a necessary upper limit to GPP/|ER|. For example, high rates of GPP will result in higher ER because of the combination of associated respiration of the autotrophs along with heterotrophic organisms contained in stream biofilms. The fraction of GPP, that is, autotrophic respiration (AR), will determine this upper limit; given a mean fraction of GPP respired each day (AR_f) of 0.44 (Hall and Beaulieu 2013), we calculate that $GPP/|ER| = GPP/(GPP \times 0.44) = 2.2$. Thus, we predict that the upper limit of GPP/|ER| is 2.2 because, on average, 44% of GPP constitutes daily autotrophic respiration. Indeed, only 1.1% of GPP/|ER| values exceeded 2.2, suggesting that this value may represent an upper bound for autotrophy in rivers.

Gas Exchange

The 14 rivers had variable gas exchange and river slope was the primary predictor of gas exchange velocity (k_{600}, Figure 4); gas exchange was lowest in Bear River, UT which had gas exchange similar to a low-wind lake (Cole and Caraco 1998). Gas exchange was highest in the Henry's Fork, which at 71 cm h^{-1} approached that of the steep, whitewater section of the Colorado through Grand Canyon (Hall and others 2012). The slope of the regression line between river slope and k_{600} was lower for these 14 rivers than for multiple measurements in the Colorado River in Grand Canyon (Hall and others 2012), likely due to the broad range of reaches through the Grand Canyon, ranging from nearly still to extremely turbulent rapids. Our 14 rivers here did not display this within-river variation in river morphology, even for the pool-drop section of the Green River in Gray Canyon. Nevertheless, gas exchange predicted using empirical equations matched closely with our data, even more closely than the original data used to derive these equations (Raymond and others 2012).

There is much interest in understanding gas exchange in rivers to estimate global gas fluxes (Raymond and others 2013). With this study, we show that across a few medium-sized continental

rivers, gas exchange can vary widely. For the purposes of an accurate metabolism estimate, it is necessary to estimate gas exchange for each river because the log–log relationship in Figure 4 has twofold prediction error. Optimistically, with high GPP and low rates of O_2 turnover (K_{600}), it is possible to model gas exchange using solely O_2 data, with no need to perform an experimental gas tracer addition (for example, SF_6) in these rivers. For the purposes of scaling gas exchange, where it is impractical to empirically measure gas exchange for an entire river network, the method employed by Raymond and others (2012) is likely the best available for these medium-sized rivers in the sense that it is unbiased (though with large prediction error) and captures much of the variability in k_{600}.

C Spiraling

Spiraling lengths for OC were generally long, but variable, in these 14 rivers. In 7 cases, S_{OC} was shorter than the length of the river segment that we measured, suggesting that there can be complete turnover of the OC pool along the length of some rivers. Functionally, rivers with an S_{OC} roughly equal to segment length have turned over more than 50% of the OC pool in that length, although a caveat to this conclusion is that we evaluated these rivers at baseflow discharge. High flows associated with storms or snowmelt would assuredly result in much longer OC spiraling lengths because the OC flux would increase more than any increase in organic matter processing (that is, HR) during high flow periods. Notably, the singular aspect of C cycling that most C spiraling studies (ours and others) generally overlook is that most OC transport will occur during periods of high flow, resulting in substantial intra-annual variation in S_{OC} (Meyer and Edwards 1990). However, our analysis shows that, at least at baseflow, heterotrophic activity can drive substantial mineralization of OC along a river's length. Given scaling relationships between element spiraling length and river length, a constant v_{f-OC} means that spiraling length increases less than proportionally with downstream distance from headwaters (Hall and others 2013). We suggest that OC mineralization and subsequent turnover of OC pools occurs to the same degree in larger streams and rivers as in the more well-studied small streams.

It is important to note that although GPP/|ER| is higher in rivers than headwaters, it is clear that there is substantial processing of allochthonous C in rivers supported by the high rates of HR across a range of stream and river sizes (Figure 3). This point has also been noted previously by Cole and Caraco (2001) for large rivers; these findings suggest that rivers are important sites for the mineralization for OC. Alternatively, this ''allochthonous'' C fueling excess ER downstream could be C produced via autochthonous production that is subsequently transported, and then mineralized, in downstream river segments (Genzoli and Hall, unpublished data).

From the perspective of C cycling, data from these 14 rivers combined with that from the literature support that rivers are reactive ecosystems. With the current interest in examining how freshwater ecosystems contribute to regional and global C budgets (Battin and others 2008, 2009; Raymond and others 2013), we suggest that rivers may strongly influence mineralization and fixation of new C in addition to their more obvious role in the longitudinal transport of C. In fact at baseflow, mineralization and transport are balanced such that OC can turn over completely in some river reaches. In rivers without substantial groundwater inputs containing terrestrial sources of dissolved CO_2, we may expect that net ecosystem production (NEP) for rivers will roughly equal CO_2 emissions, as has been found for the Hudson River (Cole and Caraco 2001). Metabolism and C spiraling data from this study represent an approach to examine the biogeochemical mechanisms controlling riverine C cycling, but only represent a snapshot in time. In the future, we expect that time series of metabolism data will provide estimates across a range of seasonal and hydrologic conditions, supporting a more thorough understanding of the role of rivers in C cycling.

ACKNOWLEDGEMENTS

We heartily thank the River Gypsies, our trusty band of hard workers who helped immensely in our field campaigns between 2010 and 2012: CD Baxter, HA Bechtold, K Dahl, J Davis, LA Genzoli, MR Grace, SA Gregory, B Hanrahan, CF Johnson, D Kincaid, U Mahl, MM Miller, JD Ostermiller, D Oviedo, JD Reed, AJ Reisinger, T Royer, C Ruiz, E Salmon-Taylor, AL Saville, A Shogren, MR Schroer, MR Shupryt, and IJ Washbourne. U Mahl and I Washbourne measured solute concentrations. S. Ye calculated the lengths of rivers. RA Payn helped define the 2-station model. HL Madinger analyzed argon concentrations. We thank DE Schindler and two anonymous reviewers for comments greatly improving this paper. We also gratefully acknowledge a collaborative grant from the National Science Foundation that supported

our research (DEB 09-21598, 09-22153, 09-22118, 10-07807).

REFERENCES

APHA. 1998. Standard methods for the examination of water and wastewater. 20th edn. Washington, DC: American Public Health Association.

Battin T, Kaplan L, Findlay S, Hopkinson C, Marti E, Packman A, Newbold J, Sabater F. 2008. Biophysical controls on organic carbon fluxes in fluvial networks. Nat Geosci 1:95–100.

Battin TJ, Luyssaert S, Kaplan LA, Aufdenkampe AK, Richter A, Tranvik LJ. 2009. The boundless carbon cycle. Nat Geosci 2:598–600.

Beaulieu JJ, Arango CP, Balz DA, Shuster WD. 2013. Continuous monitoring reveals multiple controls on ecosystem metabolism in a suburban stream. Freshw Biol 58:918–37.

Bernot MJ, Sobota DJ, Hall RO, Mulholland PJ, Dodds WK, Webster JR, Tank JL, Ashkenas LR, Cooper LW, Dahm CN, Gregory SV, Grimm NB, Hamilton SK, Johnson SL, McDowell WH, Meyer JL, Peterson BJ, Poole GC, Valett HM, Arango CP, Beaulieu JJ, Burgin AJ, Crenshaw C, Helton AM, Johnson LT, Merriam J, Niederlehner BR, O'Brien JM, Potter JD, Sheibley RW, Thomas SM, Wilson K. 2010. Inter-regional comparison of land-use effects on stream metabolism. Freshw Biol 55:1874–90.

Chapra SC, Di Toro DM. 1991. Delta method for estimating primary production, respiration, and reaeration in streams. J Environ Eng 117:640–55.

Colangelo DJ. 2007. Response of river metabolism to restoration of flow in the Kissimmee River, Florida, USA. Fresh Biol 52:459–70.

Cole JJ, Caraco NF. 1998. Atmospheric exchange of carbon dioxide in a low-wind oligotrophic lake measured by the addition of SF_6. Limnol Oceanogr 43:647–56.

Cole JJ, Caraco NF. 2001. Carbon in catchments: connecting terrestrial carbon losses with aquatic metabolism. Mar Freshw Res 52:101–10.

Cross WF, Baxter CV, Rosi-Marshall EJ, Hall RO, Kennedy TA, Donner KC, Wellard Kelly HA, Seegert SEZ, Behn KE, Yard MD. 2013. Food-web dynamics in a large river discontinuum. Ecol Monogr 83:311–37.

Davis CJ, Fritsen CH, Wirthlin ED, Memmott JC. 2012. High rates of primary productivity in a semi-arid tailwater: implications for self-regulated production. River Res Appl 28:1820–9.

Dodds WK, Veach AM, Ruffing CM, Larson DM. 2013. Abiotic controls and temporal variability of river metabolism: multiyear analyses of Mississippi and Chattahoochee River data. Freshw Sci 32:1073–87.

Finlay J. 2011. Stream size and human influences on ecosystem production in river networks. Ecosphere 2:art87. doi:10.1890/ES11-00071.1.

Genzoli LA, Hall RO. In revision. Shifts in Klamath River metabolism following a reservoir cyanobacterial bloom. Freshw Sci.

Geyer CJ, Johnson LT. 2013. MCMC: Markov chain Monte Carlo. Package version 0.9-2. http://www.stat.umn.edu/geyer/mcmc/.

Griffiths NA, Tank JL, Royer TV, Warrner TJ, Frauendorf TC, Rosi-Marshall EJ, Whiles MR. 2012. Temporal variation in organic carbon spiraling in Midwestern agricultural streams. Biogeochemistry 108:149–69.

Hall RO, Baker MA, Rosi-Marshall EJ, Tank JL. 2013. Solute specific scaling of inorganic nitrogen and phosphorus uptake in streams. Biogeosciences 10:7323–31.

Hall RO, Beaulieu JJ. 2013. Estimating autotrophic respiration in streams using daily metabolism data. Freshw Sci 32:507–16.

Hall RO, Kennedy TA, Rosi-Marshall EJ. 2012. Air-water oxygen exchange in a large whitewater river. Limnol Oceanogr Fluids Environ 2:1–11.

Hall RO, Tank JL, Dybdahl M. 2003. Exotic snails dominate nitrogen and carbon cycling in a highly productive stream. Front Ecol Environ 1:407–11.

Hall RO, Yackulic CB, Kennedy TA, Yard MD, Rosi-Marshall EJ, Voichick N, Behn KE. 2015. Turbidity, light, temperature, and hydropeaking control daily variation in primary production in the Colorado River, Grand Canyon. Limnol Oceanogr 60:512–26.

Heffernan JB, Cohen MJ. 2010. Direct and indirect coupling of primary production and diel nitrate dynamics in a subtropical spring-fed river. Limnol Oceanogr 55:677–88.

Holtgrieve GW, Schindler DE, Branch TA. 2010. Simultaneous quantification of aquatic ecosystem metabolism and reaeration using a Bayesian statistical model of oxygen dynamics. Limnol Oceanogr 55:1047–63.

Hornberger GM, Kelly MG. 1975. Atmospheric reaeration in a river using productivity analysis. J Environ Eng Div 101:729–39.

Huryn AD, Benstead JP, Parker SM. 2014. Seasonal changes in light availability modify the temperature dependence of ecosystem metabolism in an arctic stream. Ecology 95:2826–39.

Jähne B, Haußecker H. 1998. Air-water gas exchange. Annu Rev Fluid Mech 30:443–68.

Jankowski K, Schindler DE, Lisi PJ. 2014. Temperature sensitivity of community respiration rates in streams is associated with watershed geomorphic features. Ecology 95:2707–14.

Marcarelli AM, Baxter CV, Mineau MM, Hall RO. 2011. Quantity and quality: unifying food web and ecosystem perspectives on the role of resource subsidies in freshwaters. Ecology 92:1215–25.

McTammany ME, Webster JR, Benfield EF, Neatrour MA. 2003. Longitudinal patterns of metabolism in a southern Appalachian river. J N Am Benthol Soc 22:359–70.

Meyer JL, Edwards RT. 1990. Ecosystem metabolism and turnover of organic carbon along a blackwater river continuum. Ecology 71:668–77.

Murphy J, Riley JP. 1962. A modified single solution method for the determination of phosphate in natural waters. Anal Chim Acta 27:31–6.

Newbold JD, Mulholland PJ, Elwood JW, O'Neill RV. 1982. Organic carbon spiralling in stream ecosystems. Oikos 38:266–72.

Odum HT. 1957. Trophic structure and productivity of Silver Springs, Florida. Ecol Monogr 27:55–112.

R Development Core Team. 2011. R: A language and environment for statistical computing. Vienna: R Foundation for Statistical Computing http://www.R-project.org/.

Raymond PA, Hartmann J, Lauerwald R, Sobek S, McDonald CP, Hoover M, Butman D, Striegl R, Mayorga E, Humborg C, Kortelainen P, Dürr H, Meybeck M, Cais P, Guth P. 2013.

Global carbon dioxide emissions from inland waters. Nature 503:355–9.

Raymond PA, Zappa CJ, Butman D, Bott TL, Potter J, Mulholland P, Laursen AE, McDowell WH, Newbold D. 2012. Scaling the gas transfer velocity and hydraulic geometry in streams and small rivers. Limnol Oceanogr Fluids Environ 2:41–53.

Reichert P, Uehlinger U, Acuña V. 2009. Estimating stream metabolism from oxygen concentrations: effect of spatial heterogeneity. J Geophys Res Biogeosci 114:G03016. doi:10.1029/2008JG000917.

Roberts BJ, Mulholland PJ, Hill WR. 2007. Multiple scales of temporal variability in ecosystem metabolism rates: results from 2 years of continuous monitoring in a forested headwater stream. Ecosystems 10:588–606.

Roley SS, Tank JL, Griffiths NA, Hall RO, Davis RT. 2014. The influence of floodplain restoration on whole-stream metabolism in an agricultural stream: insights from a 5-year continuous dataset. Freshw Sci 33:1043–59.

Solorzano L. 1969. Determination of ammonia in natural water by the phenolhypochlorite method. Limnol Oceanogr 14:799–801.

Staehr PA, Baastrup-Spohr L, Sand-Jensen K, Stedmon C. 2012. Lake metabolism scales with lake morphometry and catchment conditions. Aquat Sci 74:155–69.

Taylor BW, Flecker AS, Hall RO. 2006. Loss of a harvested fish species disrupts carbon flow in a diverse tropical river. Science 313:833–6.

Thomas S, Royer T, Snyder E, Davis J. 2005. Organic carbon spiraling in an Idaho river. Aquat Sci 67:424–33.

Thorp JH, Delong MD. 2002. Dominance of autochthonous autotrophic carbon in food webs of heterotrophic rivers. Oikos 96:543–50.

Tranvik LJ, Downing JA, Cotner JB, Loiselle SA, Striegl RG, Ballatore TJ, Dillon P, Finlay K, Fortino K, Knoll LB. 2009. Lakes and reservoirs as regulators of carbon cycling and climate. Limnol Oceanogr 54:2298–314.

Trexler JC, Travis J. 1993. Nontraditional regression analyses. Ecology 74:1629–37.

Uehlinger U. 2006. Annual cycle and inter-annual variability of gross primary production and ecosystem respiration in a flood-prone river during a 15-year period. Freshw Biol 51:938–50.

Van de Bogert MC, Carpenter SR, Cole JJ, Pace ML. 2007. Assessing pelagic and benthic metabolism using free water measurements. Limnol Oceanogr Methods 5:145–55.

Vannote RL, Minshall GW, Cummins KW, Sedell JR, Cushing CE. 1980. The river continuum concept. Can J Fish Aquat Sci 37:130–7.

Webster JR. 2007. Spiraling down the river continuum: stream ecology and the U-shaped curve. J N Am Benthol Soc 26:375–89.

Wetzels R, Wagenmakers E-J. 2012. A default Bayesian hypothesis test for correlations and partial correlations. Psychon Bull Rev 19:1057–64.